ELSEVIER

Journal of Nuclear Materials 249 (1997) 207–222

journal of nuclear materials

The analytical and numerical study of the fluorination of uranium dioxide particles

S.S. Sazhin [a,*], A.P. Jeapes [b]

[a] *Department of Mechanical and Manufacturing Engineering, University of Brighton, Cockcroft Building, Moulsecoomb, Brighton BN2 4GL, UK*

[b] *BNFL, Sellafield, Seaside, Cumbria CA20 1PG, UK*

Received 17 October 1996; accepted 4 June 1997

Abstract

A detailed analytical study of the equations describing the fluorination of UO_2 particles is presented for some limiting cases assuming that the mass flowrate of these particles is so small that they do not affect the state of the gas. The analytical solutions obtained can be used for approximate estimates of the effect of fluorination on particle diameter and temperature but their major application, however, is probably in the verification of self-consistent numerical solutions. Computational results are presented and discussed for a self-consistent problem in which both the effects of gas on particles and particles on gas are accounted for. It has been shown that in the limiting cases for which analytical solutions have been obtained, the coincidence between numerical and analytical results is almost exact. This can be considered as a verification of both the analytical and numerical solutions. © 1997 Elsevier Science B.V.

1. Introduction

The chemical reaction of fluorine (F_2) and uranium dioxide (UO_2) leading to the production of uranium hexafluoride (UF_6) has been extensively studied for many years (see, for example, Yahata and Iwasaki [1], Iwasaki [2], Sakurai [3,4]). As a result, basic properties of this reaction (including temperature dependence) have been established experimentally, using UO_2 pellets (Iwasaki [2]) and UO_2 powder (Sakurai [3]). However, before the results of these authors could be used for optimising the technological process of UF_6 production, a number of questions need to be answered. These include such questions as: ''How does the temperatures of gas and UO_2 change during the reaction in an environment which is different from that used in the experiments of the above mentioned authors?'', ''How does the mass of UO_2 powder or pellets change during the reaction in this environment?'', ''How is the change in temperature of UO_2 powder or pellets related to the change in their mass?''.

These questions can be answered either by performing the relevant experiments or by means of a computer simulation of the heat and mass balance of chemically reacting UO_2 powder or pellets. The second approach is certainly less costly than the first. In fact the results of computer simulations would help in the optimizing of experimental setups. In some cases it appears to be very helpful to forecast the results of numerical simulations for some limiting cases by means of relatively simple analytical solutions. These solutions could enable us to determine the general properties of the phenomenon and they can be used to make an initial choice of parameters for computer simulations.

* Corresponding author. Fax: +44-1273 642 301.

PII S0022-3115(97)00229-8

The aim of this paper is to present some of the analytical solutions of the basic conservation equations describing chemically reacting UO_2 particles (which would in a certain sense incorporate powder and pellets) and to compare these solutions with the results of numerical simulations.

In Section 2 we describe the basic properties of the reaction between UO_2 and F_2 as inferred from the experimental results reported by Iwasaki [2] and Sakurai [3,4]. The basic equations and approximations used in our model are presented and discussed in Section 3. In Section 4 we present analytical solutions of these equations for some limiting cases. In Section 5 these solutions are compared with the results of numerical solutions for some of these cases. The results of numerical simulations for a more realistic case are presented in Section 6. The main conclusions of the paper are summarized in Section 7.

2. Chemical reaction

The fluorination of uranium dioxide can be subdivided into 2 main steps. Firstly

$$UO_2(\text{solid}) + F_2(\text{gas}) \rightarrow UO_2F_2(\text{surface}) \tag{2.1}$$

(chemisorption of fluorine), secondly

$$UO_2F_2(\text{surface}) + 2F_2(\text{gas}) \rightarrow UF_6(\text{gas}) + O_2(\text{gas}). \tag{2.2}$$

In the case of UO_2 pellets, Iwasaki [2] separates the process:

$$UO_2(\text{pellets}) \rightarrow UO_2(\text{partly fluorinated powder}) \tag{2.3}$$

which precedes the reaction (Eq. (2.1)) forming UO_2F_2 powder.

The combination of reactions Eqs. (2.1) and (2.2) is accompanied by a free energy increase at the rate of 244.5 kcal/mol (Sakurai [3,4]). This free energy increase due to the chemical reaction is equal to the enthalpy of the reaction and the heat of reaction (H_{reac}) (see Ref. [5], pp. 31, 47).

Processes Eqs. (2.3) and (2.2) are surface reactions which proceed at the interface between the pellet core and the intermediate layer (partly fluorinated UO_2F_2 powder) and on the outside of this intermediate layer respectively, whereas process Eq. (2.1) proceeds throughout the intermediate layer. At temperatures below 430°C the rate of reaction Eq. (2.2) is negligible, so that the fluorination results in the production of UO_2F_2 powder only. Above 430°C the rate of reaction Eq. (2.2) increases and the quantity of the intermediate UO_2F_2 powder begins to reduce. We will restrict our analysis to temperatures above 430°C which allows us to reduce reactions Eqs. (2.1), (2.2) and (2.3) to a single surface reaction:

$$UO_2 + 3F_2 \rightarrow UF_6 + O_2, \quad H_{\text{reac}} = 244.5 \text{ kcal/mol} = 3.789 \times 10^6 \text{ J/kg } (UO_2). \tag{2.4}$$

Rates of reaction Eq. (2.4) (k) measured in mm/h and g/(cm^2 h) at different temperatures are shown in Table 1 based on experimental results by Iwasaki [2].

Based on the results presented in Table 1, Iwasaki [2] drew attention to the fact that the temperature dependence of k at temperatures above about 450°C can be approximated as (see his fig. 8)

$$\log_{10}\left(100k\left(\frac{\text{mm}}{\text{h}}\right)\right) \approx -\frac{4737}{T(\text{K})} + 7.384. \tag{2.5}$$

Eq. (2.5) is simply an analytical approximation of the line 'B' in fig. 8 of Iwasaki [2]. When deriving this equation we took into account that, for this line,

$$\begin{aligned} &\log_{10}\left(100k\left(\frac{\text{mm}}{\text{h}}\right)\right) = 1.7 \quad \text{when } 1000/T(\text{K}) = 1.20, \\ &\log_{10}\left(100k\left(\frac{\text{mm}}{\text{h}}\right)\right) = 0.8 \quad \text{when } 1000/T(\text{K}) = 1.39. \end{aligned} \tag{2.6}$$

Taking the density of UO_2 (ρ_{UO_2}) equal to 10.53 g/cm^3, Eq. (2.5) can be rewritten as

$$k\left(\frac{\text{kg}}{\text{m}^2\,\text{s}}\right) = a\exp\left(-\frac{b}{T(\text{K})}\right), \tag{2.7}$$

where $a = 708.15$ and $b = 10907$.

Eq. (2.7) represents the well known Arrhenius law (see Kuo [5]).

Table 1
Experimental reaction rate constants

Temperature (C)	k (mm/h)	k (g/cm^2 h)
460	0.081	0.085
480	0.104	0.109
500	0.200	0.210
520	0.278	0.292
540	0.380	0.400

Results presented in Table 1 on which Eq. (2.7) was based were obtained in the experiment when the partial pressure of F_2 was 152 mm Hg, i.e., the fluorine concentration was 20% by volume. For an arbitrary fluorine concentration this equation can be generalized to

$$k\left(\frac{\text{kg}}{\text{m}^2\,\text{s}}\right) = \alpha p_{F_2}^{\gamma}\exp(-b/T(\text{K})), \tag{2.8}$$

where p_{F_2} is the relative partial pressure (volume or mole fraction) of F_2,

$$\alpha = 7917, \quad b = 10907, \quad \gamma = 1.5. \tag{2.9}$$

When deriving the value of γ we took into account the dependence of k on p_{F_2} as reported by Yahata and Iwasaki [1] (see their Table 3). This value is not particularly reliable and can vary from 1.3 to 2.0 depending on the value of p_{F_2}. The value of α is chosen in such a way that $\alpha(0.2)^{1.5} = a = 708.15$.

3. Basic equations and approximations

In this section we summarise the main new equations and approximations used in the numerical and analytical modelling of the fluorination of UO_2 particles. Approximations used in analytical modelling but relaxed in the general numerical modelling will be specified.

Assuming that particles are perfect spheres, the mass conservation equation for them can be written as

$$\frac{\mathrm{d}m_p}{\mathrm{d}t} = -k\pi D_p^2, \tag{3.1}$$

where m_p is a particle's mass, D_p is the particle diameter and k is the reaction rate as defined by Eq. (2.8).

To simplify our analysis, we can assume that the particles do not affect the concentration of F_2 in the gas so that we can set

$$\tilde{\alpha} = \alpha p_{F_2}^{\gamma} = \text{const}. \tag{3.2}$$

This assumption will be later relaxed when we consider a coupled self-consistent solution in Section 6.

The small particle size allows us to assume that the temperature inside them is constant and equal to the temperature at the surface. As a result T in Eq. (2.8) can be assumed equal to T_p (particles' temperature). We assume that all particles are identical which allows us to restrict our analysis to one particle only.

In view of these assumptions Eq. (3.1) can be simplified to

$$\frac{\mathrm{d}D_p}{\mathrm{d}t} = -\kappa\exp\left(-\frac{b}{T_p}\right), \tag{3.3}$$

where

$$\kappa = 2\tilde{\alpha}/\rho_{UO_2}.$$

Eq. (3.3) means that the rate of change of a particle's diameter D_p is a function of T_p but does not depend on D_p.

The value of T_P in its turn can be obtained from the particle heat balance equation which we present in the form

$$m_p c_p \frac{\mathrm{d}T_p}{\mathrm{d}t} = h_c S_p(T_\infty - T_p) - f_h\frac{\mathrm{d}m_p}{\mathrm{d}t}H_{reac} + S_p\epsilon_p\sigma\left(\theta_R^4 - T_p^4\right), \tag{3.4}$$

where c_p is the particle's specific heat capacity, h_c is the convective heat transfer coefficient, S_p is the surface area of the particle, T_∞ is the gas temperature away from the particle, H_{reac} is the heat of reaction, f_h is the fraction of H_{reac} absorbed by particles, ϵ_p is the particle's emissivity, $\sigma = 5.67051 \times 10^{-8}$ W/(m^2 K^4) is the Stefan–Boltzmann constant, and θ_R is the so called radiation temperature (Pomraning and Foglesong [6]).

h_c in Eq. (3.4) can be defined as (Bird et al. [7])

$$h_c = \lambda_g \mathrm{Nu}/D_p, \tag{3.5}$$

where λ_g is the thermal conductivity of surrounding gas away from the particle, $\mathrm{Nu} = 2.0 + 0.6\mathrm{Re}_D^{1/2}\mathrm{Pr}^{1/3}$ is the Nusselt number, Re_D is the Reynolds number, and Pr is the Prandtl number.

The Reynolds and Prandtl numbers are defined as (Landau and Lifshitz [8])

$$\mathrm{Re}_D = \frac{\rho_{gas} u_{gas-particle} l_{particle}}{\eta_{gas}} = \frac{u_{gas-particle} l_{particle}}{\nu_{gas}}, \qquad \mathrm{Pr} = \frac{\nu_{gas}}{\chi_{gas}},$$

where ρ_{gas} is the gas density, $u_{gas-particle}$ is the relative velocity between gas and particles, η_{gas} is the dynamic viscosity, ν_{gas} is the kinematic viscosity, $\chi_{gas} = \kappa_{gas}/\rho_{gas}c_p$ is thermometric conductivity (thermal diffusivity), and $l_{particle}$ is the characteristic size of particles ($l_{particle} = D_p$ in the case of spheres).

When deriving Eq. (3.4) we used the so called $P-1$ model for the thermal radiation transfer which appears to be particularly convenient for quantitative analysis of radiation transfer between particles and surrounding gas (see Siegel and Howell [9]; Sazhin et al. [10]).

Following our previous assumption that the influence of particles on gas is small we can assume that neither T_∞ nor θ_R change during the course of reaction. Also we assume that the relative velocity between the particles and the gas is so small that we can assume in our analytical work that $\mathrm{Nu} = 2$ (or at least ignore the dependence of Re_D on D_p, t, and T_p). To simplify the analysis λ_g, c_p and ϵ_p can also assumed to be constant. All these assumptions will be relaxed in self-consistent computations presented and discussed in Section 6.

In view of Eqs. (3.1) and (3.5), Eq. (3.4) can be rearranged to

$$D_p^3 \frac{dT_p}{dt} = a_1 D_p(T_\infty - T_p) + a_2 D_p^2 \exp\left(-\frac{b}{T_p}\right) + a_3 D_p^2(\theta_R^4 - T_p^4), \tag{3.6}$$

where

$$a_1 = \frac{6\lambda_g \mathrm{Nu}}{c_p \rho_{UO_2}}, \qquad a_2 = \frac{6 f_h H_{reac} \tilde{\alpha}}{c_p \rho_{UO_2}}, \qquad a_3 = \frac{6\epsilon_p \sigma}{c_p \rho_{UO_2}}. \tag{3.7}$$

The system of Eqs. (3.3) and (3.6) need to be solved numerically in general. In some limiting cases, however, analytical solutions of this system appear to be possible. These cases will be considered in Section 4.

4. Analytical solutions

If we know the time dependence of T_p then the analytical solution of Eq. (3.3) appears to be straightforward. On the other hand the analytical solution of Eq. (3.6) with respect to T_p appears not to be obvious even if D_p as a function of t is known. In what follows we will look for the solution of the system Eqs. (3.3) and (3.6) in the form $D_p(T_p)$, which will predict the change of particles' sizes depending on their temperature. An analytical solution in this form appears to be possible in two limiting cases: one when the change in T_p is predominantly due to the thermal conduction in the gas (the first term on the right hand side of Eq. (3.6) is the dominant one); the other when change in T_p is predominantly due to the heat of reaction and thermal radiation (the last two terms on the right hand side of Eq. (3.6) are the dominant ones). These two limiting cases will be considered separately in Sections 4.1 and 4.2.

4.1. Contributions of the heat of reaction and thermal radiation are small

If the contribution of the heat of reaction and thermal radiation are small then we can ignore the contribution of the last two terms in the right hand side of Eq. (3.6) and simplify this equation to

$$\frac{dT_p}{dt} = \frac{a_1(T_\infty - T_p)}{D_p^2}. \tag{4.1}$$

Dividing Eq. (4.1) by Eq. (3.3), we obtain

$$\frac{dT_p}{dD_p} = -\frac{a_1(T_\infty - T_p)}{\kappa D_p^2}\exp\left(\frac{b}{T_p}\right). \tag{4.2}$$

The solution of Eq. (4.2) can be presented as

$$D_p = \left[\frac{1}{D_{p0}} - \frac{\kappa}{a_1}\int_{1/T_{p0}}^{1/T_p}\frac{dx\exp(-bx)}{x^2T_\infty - x}\right]^{-1}, \tag{4.3}$$

where T_{p0} and D_{p0} are a particle's initial temperature and diameter.

It is easy to see that in both cases when $T_\infty > T_p$ and $T_\infty < T_p$ we have $D_p < D_{p0}$. The solution Eq. (4.3) fails when $T_\infty = T_{p0}$. In this case, however, the solution of Eqs. (3.3) and (4.1) is trivial: $D_p = \text{const}$ and $T_p = \text{const}$ (no heat transfer takes place).

Eq. (4.3) can be regarded as the required explicit analytical solution of the system of Eqs. (3.3) and (3.6). Unfortunately, however, the integral on the right hand side of Eq. (4.3) cannot be expressed in terms of elementary or known special functions. This presentation appears to be possible in two limiting cases: when the temperature of surrounding gas T_∞, is well above or well below the particle's temperature T_p. These are the most likely cases when the contribution of thermal conduction is particularly important.

(a) $T_\infty \gg T_p$.

In this case Eq. (4.3) can be simplified to

$$D_p = \left[\frac{1}{D_{p0}} - \frac{\kappa}{a_1T_\infty}\int_{1/T_{p0}}^{1/T_p}\frac{dx\exp(-bx)}{x^2} - \frac{\kappa}{a_1T_\infty^2}\int_{1/T_{p0}}^{1/T_p}\frac{dx\exp(-bx)}{x^3}\right]^{-1}. \tag{4.4}$$

Remembering the definition of $\mathrm{Ei}(x)$:

$$\begin{aligned}\mathrm{Ei}(x) &= \int_{-\infty}^{x}\frac{\exp t}{t}dt \qquad \text{when } x<0,\\ \mathrm{Ei}(x) &= -\lim_{\epsilon\to+0}\left[\int_{-x}^{-\epsilon}\frac{\exp -t}{t}dt + \int_{\epsilon}^{\infty}\frac{\exp -t}{t}dt\right] \qquad \text{when } x>0,\end{aligned} \tag{4.5}$$

we can rearrange Eq. (4.4) to (see Gradstein and Ryzhik [11])

$$\begin{aligned}D_p = \Bigg[\frac{1}{D_{p0}} &- \left(-\frac{\kappa T_p}{a_1T_\infty} - \frac{\kappa T_p^2}{2a_1T_\infty^2} + \frac{b\kappa T_p}{2a_1T_\infty^2}\right)\exp\left(-\frac{b}{T_p}\right) - \left(\frac{\kappa T_{p0}}{a_1T_\infty} + \frac{kT_{p0}^2}{2a_1T_\infty^2} - \frac{b\kappa T_{p0}}{2a_1T_\infty^2}\right)\exp\left(-\frac{b}{T_{p0}}\right)\\ &- \left(-\frac{b\kappa}{a_1T_\infty} + \frac{b^2\kappa}{2a_1T_\infty^2}\right)\left(\mathrm{Ei}\left(-\frac{b}{T_p}\right) - \mathrm{Ei}\left(-\frac{b}{T_{p0}}\right)\right)\Bigg]^{-1}.\end{aligned} \tag{4.6}$$

Note that in both cases, $x<0$ and $x>0$, $\mathrm{Ei}(x)$ can be expanded as

$$\mathrm{Ei}(x) = \gamma + \ln|x| + \sum_{n=1}^{\infty}\frac{x^n}{n\cdot n!}, \tag{4.5'}$$

where $\gamma = 0.5772156$ is the Euler constant.

For large and positive x we can use the following asymptotic expansion (Gradstein and Ryzhik [10])

$$\mathrm{Ei}(-x) = \exp(-x)\sum_{k=1}^{n}(-1)^k\frac{(k-1)!}{x^k} + R_n, \tag{4.5''}$$

where

$$R_n < \frac{n!}{x^{n+1}}.$$

For most realistic values of temperature, we have $b/T_p \gg 1$ which allows us to use just the first two terms in the expansion Eq. (4.5″) and simplify Eq. (4.6) to

$$D_p = \left[\frac{1}{D_{p0}} + \frac{\kappa}{a_1bT_\infty}\left(T_p^2\exp\left(-\frac{b}{T_p}\right) - T_{p0}^2\exp\left(-\frac{b}{T_{p0}}\right)\right)\right]^{-1}. \tag{4.6'}$$

(b) $T_\infty \ll T_p$.

This case (cooling of particles) is less realistic for practical applications but we will consider it for completeness of our analysis. Keeping only linear terms, Eq. (4.4) can be simplified to

$$D_p = \left[\frac{1}{D_{p0}} + \frac{\kappa}{a_1}\int_{1/T_{p0}}^{1/T_p}\frac{dx\exp(-bx)}{x} + \frac{\kappa T_\infty}{a_1}\int_{1/T_{p0}}^{1/T_p} dx\exp(-bx)\right]^{-1}. \tag{4.7}$$

In view of Eq. (4.5), Eq. (4.7) can be rearranged to

$$D_p = \left[\frac{1}{D_{p0}} + \frac{\kappa}{a_1}\left(\mathrm{Ei}\left(-\frac{b}{T_p}\right) - \mathrm{Ei}\left(-\frac{b}{T_{p0}}\right)\right) - \frac{\kappa T_\infty}{a_1 b}\left[\exp\left(-\frac{b}{T_p}\right) - \exp\left(-\frac{b}{T_{p0}}\right)\right]\right]^{-1}. \tag{4.8}$$

Solutions Eqs. (4.6) and (4.8) can be used to obtain higher order solutions of Eq. (3.6) (taking into account the small contribution of the last two terms in the right hand side of Eq. (3.6)). These solutions, however, turned out to be too complicated for any practical applications.

4.2. Contribution of thermal conduction is small

If the contribution of thermal conduction is small then we can ignore the contribution of the first term in the right hand side of Eq. (3.6) and simplify this equation to

$$\frac{dT_p}{dt} = \frac{1}{D_p}\left[a_2\exp\left(-\frac{b}{T_p}\right) + a_3\left(\theta_R^4 - T_p^4\right)\right]. \tag{4.9}$$

Dividing Eq. (4.9) by Eq. (3.3) we obtain

$$\frac{dT_p}{dD_p} = -\frac{1}{\kappa D_p}\left[a_2 + a_3\left(\theta_R^4 - T_p^4\right)\exp\left(\frac{b}{T_p}\right)\right]. \tag{4.10}$$

The solution of Eq. (4.10) can be presented as

$$D_p = D_{p0}\exp\left[\kappa\int_{1/T_{p0}}^{1/T_p}\frac{x^2\,dx}{a_3\theta_R^4 x^4\exp(bx) - a_3\exp(bx) + a_2 x^4}\right]. \tag{4.11}$$

Although Eq. (4.11) can be regarded as the required explicit solution of the system of Eqs. (3.3) and (3.6) in the limit of small thermal conductivity, some further simplifications of this equation are required in order that $D_p(T_p)$ can be expressed in terms of elementary or known special functions. These simplifications are possible in three limiting cases when one of the terms in the denominator of the right hand side of Eq. (4.11) is dominant.

(a) Contribution of the heat of reaction is small and the radiation from the gas dominates over the radiation from the particles ($\theta_R^4 \gg T_p^4$).

In this case Eq. (4.11) can be simplified to

$$D_p = D_{p0}\exp\left[\frac{\kappa}{a_3\theta_R^4}\int_{1/T_{p0}}^{1/T_p}\frac{\exp(-bx)}{x^2}\,dx - \frac{\kappa a_2}{a_3^2\theta_R^8}\int_{1/T_{p0}}^{1/T_p}\frac{\exp(-2bx)}{x^2}\,dx + \frac{\kappa}{a_3\theta_R^8}\int_{1/T_{p0}}^{1/T_p}\frac{\exp(-bx)}{x^6}\,dx\right]. \tag{4.12}$$

Remembering Eq. (4.5) we can rearrange Eq. (4.12) to

$$\begin{aligned} D_p = D_{p0}\exp\Bigg\{ & -\frac{\kappa}{a_3\theta_R^4}\left[T_p\exp\left(-\frac{b}{T_p}\right) - T_{p0}\exp\left(-\frac{b}{T_{p0}}\right)\right] - \frac{\kappa b}{a_3\theta_R^4}\left[\mathrm{Ei}\left(-\frac{b}{T_p}\right) - \mathrm{Ei}\left(-\frac{b}{T_{p0}}\right)\right] \\ & + \frac{\kappa a_2}{a_3^2\theta_R^8}\left[T_p\exp\left(-\frac{2b}{T_p}\right) - T_{p0}\exp\left(-\frac{2b}{T_{p0}}\right)\right] + \frac{2\kappa b a_2}{a_3^2\theta_R^8}\left[\mathrm{Ei}\left(-\frac{2b}{T_p}\right) - \mathrm{Ei}\left(-\frac{2b}{T_{p0}}\right)\right] \\ & - \frac{k}{a_3\theta_R^8}\left[\exp\left(-\frac{b}{T_p}\right)\left[\frac{T_p^5}{5} - \frac{T_p^4 b}{20} + \frac{T_p^3 b^2}{60} - \frac{T_p^2 b^3}{120} + \frac{T_p b^4}{120}\right] + \frac{b^5}{5!}\mathrm{Ei}\left(-\frac{b}{T_p}\right)\right. \\ & \left. - \exp\left(-\frac{b}{T_{p0}}\right)\left[\frac{T_{p0}}{5} - \frac{T_{p0}^4 b}{20} + \frac{T_{p0}^3 b^2}{60} - \frac{T_{p0}^2 b^3}{120} + \frac{T_{p0} b^4}{120}\right] - \frac{b^5}{5!}\mathrm{Ei}\left(-\frac{b}{T_{p0}}\right)\right]\Bigg\}. \end{aligned} \tag{4.13}$$

Ignoring the contribution of quadratic terms with respect to θ_R^{-4} we can simplify Eq. (4.13) to

$$D_p = D_{p0}\exp\left\{-\frac{\kappa}{a_3\theta_R^4}\left[T_p\exp\left(-\frac{b}{T_p}\right)-T_{p0}\exp\left(-\frac{b}{T_{p0}}\right)\right]-\frac{\kappa b}{a_3\theta_R^4}\left[\mathrm{Ei}\left(-\frac{b}{T_p}\right)-\mathrm{Ei}\left(-\frac{b}{T_{p0}}\right)\right]\right\}. \tag{4.14}$$

In the case when $b \ll T_p$ we can use the asymptotic expansion Eq. (4.5″) for $\mathrm{Ei}(x)$. Taking the first two terms in this expansion we can further simplify Eq. (4.14) to

$$D_p = D_{p0}\exp\left\{-\frac{\kappa}{a_3\theta_R^4 b}\left[T_p^2\exp\left(-\frac{b}{T_p}\right)-T_{p0}^2\exp\left(-\frac{b}{T_p}\right)\right]\right\}. \tag{4.14'}$$

(b) Contribution of the heat of reaction is small and the radiation from the gas is dominated by the radiation from the particles ($\theta_R^4 \ll T_p^4$).

This case (cooling of particles) is less important for practical applications but we will consider it for completeness of our analysis (cf. Section 4.1.b). Keeping only linear terms, Eq. (4.11) can be simplified to

$$D_p = D_{p0}\exp\left[-\frac{\kappa}{a_3}\int_{1/T_{p0}}^{1/T_p}x^2\exp(-bx)\,dx-\frac{\kappa\theta_R^4}{a_3}\int_{1/T_{p0}}^{1/T_p}x^6\exp(-bx)\,dx-\frac{\kappa a_2}{a_3^2}\int_{1/T_{p0}}^{1/T_p}x^6\exp(-2bx)\,dx\right]. \tag{4.15}$$

All integrals in the right hand side of Eq. (4.15) can be expressed in terms of elementary functions. As a result this equation can be rearranged to

$$\begin{aligned}D_p = D_{p0}\exp\Bigg\{&-\frac{\kappa}{a_3}\left[\left(\frac{2}{b^3}+\frac{2}{b^2T_{p0}}+\frac{1}{bT_{p0}^2}\right)\exp\left(-\frac{b}{T_{p0}}\right)-\left(\frac{2}{b^3}+\frac{2}{b^2T_p}+\frac{1}{bT_p^2}\right)\exp\left(-\frac{b}{T_p}\right)\right]\\&+\left[\frac{6!\kappa\theta_R^4}{a_3}\sum_{n=0}^{6}\left(\frac{\exp(-b/T_p)}{b^{n+1}T_p^{6-n}(6-n)!}-\frac{\exp(-b/T_{p0})}{b^{n+1}T_{p0}^{6-n}(6-n)!}\right)\right.\\&\left.+\frac{6!\kappa a_2}{a_3^2}\sum_{n=0}^{6}\left(\frac{\exp(-2b/T_p)}{(2b)^{n+1}T_p^{6-n}(6-n)!}-\frac{\exp(-2b/T_{p0})}{(2b)^{n+1}T_{p0}^{6-n}(6-n)!}\right)\right]\Bigg\}.\end{aligned} \tag{4.16}$$

Keeping only the lowest order terms, Eq. (4.16) can be simplified to

$$D_p = D_{p0}\exp\left\{-\frac{\kappa}{a_3}\left[\left(\frac{2}{b^3}+\frac{2}{b^2T_{p0}}+\frac{1}{bT_{p0}^2}\right)\exp\left(-\frac{b}{T_{p0}}\right)-\left(\frac{2}{b^3}+\frac{2}{b^2T_p}+\frac{1}{bT_p^2}\right)\exp\left(-\frac{b}{T_p}\right)\right]\right\}. \tag{4.17}$$

(c) Contribution of radiation is small.

In this case Eq. (4.11) can be simplified to

$$D_p = D_{p0}\exp\left[-\frac{\kappa(T_p-T_{p0})}{a_2}-\frac{\kappa a_3\theta_R^4}{a_2^2}\int_{1/T_{p0}}^{1/T_p}\frac{\exp(bx)\,dx}{x^2}+\frac{\kappa a_3}{a_2^2}\int_{1/T_{p0}}^{1/T_p}\frac{\exp(bx)\,dx}{x^6}\right]. \tag{4.18}$$

In view of Eq. (4.5), Eq. (4.18) can be rearranged to

$$\begin{aligned}D_p = D_{p0}\exp\Bigg\{&-\frac{\kappa(T_p-T_{p0})}{a_2}-\frac{\kappa a_3\theta_R^4}{a_2^2}\left[T_{p0}\exp\left(\frac{b}{T_{p0}}\right)-T_p\exp\left(\frac{b}{T_p}\right)\right]\\&-\frac{\kappa a_3\theta_R^4 b}{a_2^2}\left[\mathrm{Ei}\left(\frac{b}{T_p}\right)-\mathrm{Ei}\left(\frac{b}{T_{p0}}\right)\right]-\frac{\kappa a_3}{a_2^2}\left[\exp\left(\frac{b}{T_p}\right)\left[\frac{T_p^5}{5}+\frac{T_p^4b}{20}+\frac{T_p^3b^2}{60}+\frac{T_p^2b^3}{120}+\frac{T_pb^4}{120}\right]\right.\\&\left.-\frac{b^5}{5!}\mathrm{Ei}\left(\frac{b}{T_p}\right)-\exp\left(\frac{b}{T_{p0}}\right)\left[\frac{T_{p0}^5}{5}+\frac{T_{p0}^4b}{20}+\frac{T_{p0}^3b^2}{60}+\frac{T_{p0}^2b^3}{120}+\frac{T_{p0}b^4}{120}\right]+\frac{b^5}{5!}\mathrm{Ei}\left(\frac{b}{T_{p0}}\right)\right]\Bigg\}.\end{aligned} \tag{4.19}$$

Taking the lowest order terms, Eq. (4.19) can be simplified to

$$D_p = D_{p0} \exp\left[\frac{-\kappa(T_p - T_{p0})}{a_2}\right]. \tag{4.20}$$

Eq. (4.20) means that in the absence of external sources of heat (thermal conduction or radiation) the size of particles decreases exponentially with increasing temperature.

5. Numerical solutions (limiting cases)

In this section we compare the results predicted by some simple analytical solutions presented in Section 4 with the corresponding results of the numerical analysis based on a CFD code where the general solution of Eqs. (3.3) and (3.6) has been implemented. This comparison will allow us to verify both our analytical and numerical solutions so that both these solutions could be applied with confidence to the analysis of more realistic cases. The limiting cases considered in this section involve heating UO_2 particles under the influence of thermal conduction from surrounding gas (contributions of the heat of reaction and thermal radiation are small) (Section 5.1), heating UO_2 particles under the influence of thermal radiation (contributions of the heat of reaction and thermal conduction are small) (Section 5.2), and heating UO_2 particles by the heat of reaction (effects of thermal conduction and thermal radiation are small) (Section 5.3). In the first two cases the particles are assumed to be so small that they do not affect the gas properties; in the third case gas properties are irrelevant, since gas is effectively isolated from particles.

Values of parameters used for the computations in this section have been chosen so that we can provide a meaningful comparison between numerical and analytical results. These does not necessarily illustrate actual physical environments.

5.1. Heating of UO_2 particles via thermal conduction from the surrounding gas

The analytical solution for this case is given by Eq. (4.6) or its simplified version Eq. (4.6′). As follows from the derivation of these equations given in Section 4, the main assumption on which it is based is that the last two terms on the

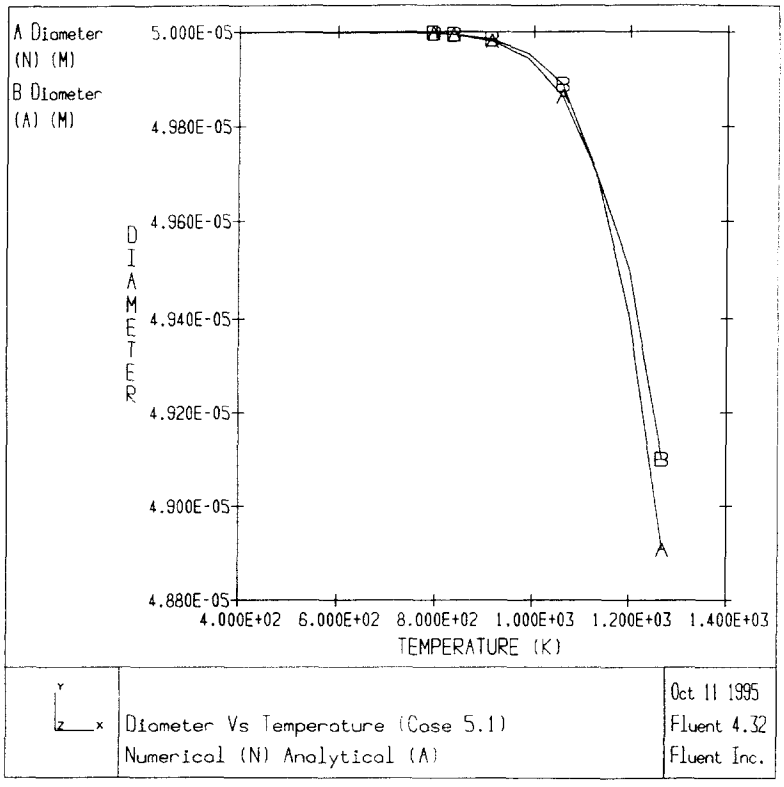

Fig. 1. Plots of particle diameter (D_p) versus particle temperature (T_p) as predicted by Eq. (4.6′) (plot B) and obtained from numerical computations (plot A) on the basis that heating of UO_2 particles is achieved via thermal conduction from the surrounding gas.

Table 2
Values of parameters used for comparison between analytical and numerical results

Parameter	Value	Units
λ_g	0.004	w/(m K)
ρ_{UO_2}	1.053 104	kg/m^3
p_{F_2}	0.5	Dimensionless
f_h	0.5	Dimensionless
Nu	2	Dimensionless
c_p	330	J/(kg K)
D_{p0}	5×10^{-5}	m
T_∞	3000	K
T_{p0}	400	K

right hand side of Eq. (3.6) can be ignored when compared with the first one. This can take place at relatively low particle temperatures T_p, when the reaction rate is small, and/or with small particle sizes. Also, the radiation temperature and/or particle emissivity need to be small.

Another condition which needs to be satisfied in order that Eqs. (4.6) and (4.6′) are valid is $T_\infty \gg T_p$. It does not seem easy to satisfy all these conditions simultaneously which means that the solutions Eqs. (4.6) and (4.6′) might be of limited practical importance. To enable us to compare these solutions with the results of numerical computations over a relatively wide range of parameters we assumed that $H_{reac} = \epsilon_p = 0$ (which guarantees the validity of Eq. (4.1)) and used the data shown in Table 2 (which guarantees the validity of the conditions: $T_\infty \gg T_p$ and $b \gg T_p$; the latter condition allows us to restrict our comparison to Eq. (4.6′)). Plots of particle diameter (D_p) versus particle temperature (T_p) as predicted by Eq. (4.6′) and obtained from numerical computations are shown in Fig. 1. As follows from this figure, the curves coincide with an error of not more than 0.5% which could be attributed to the approximate nature of Eq. (4.6′). The close agreement between the curves endorses both the analytical and numerical approaches to the problem.

5.2. Heating of UO_2 particles via thermal radiation from the surrounding gas

The analytical solution for this case is given by Eq. (4.13) or its simplified versions Eqs. (4.14) and (4.14′). Two main conditions need to be satisfied in order that this solution can be justified. Firstly, the first two terms in the right hand side of

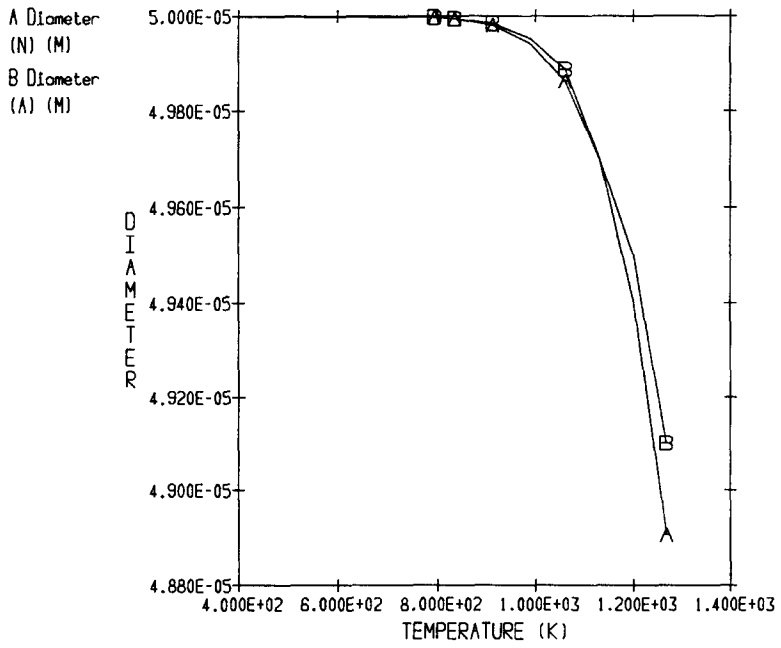

Fig. 2. Plots of particle diameter (D_p) versus particle temperature (T_p) as predicted by Eq. (4.14′) (plot B) and obtained from numerical computations (plot A) on the basis that heating of UO_2 particles is achieved via thermal radiation from the surrounding gas.

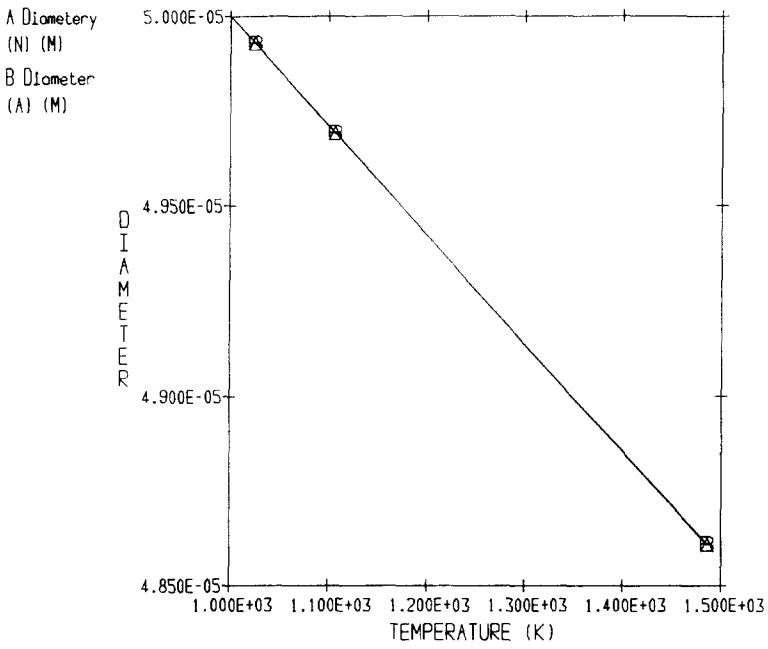

Fig. 3. Plots of particle diameter (D_p) versus particle's temperature (T_p) as predicted by Eq. (4.14′) (plot B) and obtained from numerical computations (plot A) on the basis that heating of UO_2 particles is achieved via the fluorination process.

Eq. (3.6) need to be much smaller than the third one. Secondly, the radiation temperature needs to be reasonably larger than the particle temperature so that $\theta_R^4 \gg T_p^4$. Both these conditions are satisfied by the data shown in Table 2, $\epsilon_p = 1$ and $\theta_R = 2000$ K. Indeed, for $T_p = T_{p0} = 400$ K the first term in the right hand side of Eq. (3.6) is equal to $\approx 10^{-10}$ m^3 K/s, the second term is equal to $\approx 7 \times 10^{-11}$ m^3 K/s, the third one is equal to $\approx 1.6 \times 10^{-8}$ m^3 K/s. If T_p increases to 700 K the first term would decrease, the third remains practically unchanged (decreases by about 4%), while the second would increase to $\approx 10^{-8}$ m^3 K/s with its value approaching the radiation term. Therefore this approximation can be applied in the range of T_p below 700 K. In order to compare the analytical and numerical results over a wider range of parameters ($T_p > 700$) K we assumed in our numerical computations that $H_{reac} = 0$, as was done in Section 5.1. Also we will restrict our comparison to Eq. (4.14′) only. The predictions of this equation are expected to be close to the predictions of Eqs. (4.13) and (4.14).

Plots of particle diameter (D_p) versus particle temperature (T_p) as predicted by Eq. (4.14′) and obtained from numerical computations are presented in Fig. 2 for data shown in Table 2 with $\epsilon_p = 1$ and $\theta_R = 2000$ K. The discrepancy between the curves does not exceed 0.5% which can be attributed to the approximate nature of Eq. (4.14′). As in the case of Fig. 1, the close agreement between the curves endorses both approaches to the problem.

5.3. Heating of UO_2 particles via the fluorination process

The analytical solution for this case is given by Eq. (4.20). This case can be realized when the physical and radiation temperatures of the surrounding gas are close to the particle temperature, or when both the gas thermal conductivity and particle emissivity are small. We used the following data: $D_{p0} = 10^{-4}$ m, $H_{reac} = 3.789 \times 10^6$ J/kg(UO_2) (see Section 2), $f_h = 0.5$, $c_p(UO_2) = 330$ J/(kg × K), $\lambda_g = \epsilon_p = 0$. The numerical versus analytical (based on Eq. (4.20)) plots of D_p versus T_p are shown in Fig. 3. The plots practically coincide which supports both the analytical and numerical approaches to the problem.

6. A self-consistent numerical solution

Results presented in the previous section refer to some relatively simple cases when we were able to compare numerical results with analytical solutions. The main assumption which we made was that the particles do not influence the gas flow parameters. Although those results were very important for the verification of our code, they seem to be of limited practical interest.

In this section we present a self-consistent solution to the problem, when the effects of both the gas flow on particles and particles on the gas flow are accounted for. The gas flow was treated as turbulent, and the k–ϵ turbulence model was used. Particle trajectories were calculated using mean tracks. The temperature of the wall was assumed constant and equal to 350 K.

6.1. Input parameters

The reaction takes place in a cylinder 5 m long with a radius of 0.1016 m. A mixture of UO_2 particles, F_2 and Ar is blown into the cylinder from one end and products of reaction (UF_6 and O_2) along with Ar and possible remnants of F_2 are blown out of the tube from the other end.

The mass flowrate of UO_2 particles is assumed 5.672 tonnes/day, which corresponds to

$$M_f(UO_2) = 0.0656 \text{ kg/s}. \tag{6.1}$$

We approximate the continuous flow of particles by the injection of these particles from 5 injection locations at the following radii:

$$r_1 = 0.01 \text{ m}, \quad r_2 = 0.03 \text{ m}, \quad r_3 = 0.05 \text{ m}, \quad r_4 = 0.07 \text{ m}, \quad r_5 = 0.09 \text{ m}. \tag{6.2}$$

The mass flowrates of the particles injected from these locations are taken equal to

$$M_{f1}(UO_2) = 0.0025 \text{ kg/s}, \quad M_{f2}(UO_2) = 0.0076 \text{ kg/s}, \quad M_{f3}(UO_2) = 0.0127 \text{ kg/s},$$
$$M_{f4}(UO_2) = 0.0178 \text{ kg/s}, \quad M_{f5}(UO_2) = 0.0249 \text{ kg/s}. \tag{6.3}$$

These mass flowrates are chosen in such a way as to give

$$\sum_{i=1}^{5} M_{fi}(UO_2) = 0.0655 \text{ kg/s} \tag{6.4}$$

(close to the value in Eq. (6.1)) and

$$M_{fi}(UO_2) \propto \pi\left[(r_i + 0.01 \text{ m})^2 - (r_i - 0.01 \text{ m})^2\right] \tag{6.5}$$

(mass flowrate is proportional to the corresponding fraction of the inlet area).

Remembering that the molecular weight of UO_2 is equal to

$$M(UO_2) = 270 \frac{\text{kg}}{\text{kg mol}}, \tag{6.6}$$

we obtain from Eq. (6.4) the mole flowrate of UO_2:

$$\text{Mo}_f(UO_2) = \frac{0.0655}{270} \frac{\text{kg mol}}{\text{s}} = 2.426 \times 10^{-4} \frac{\text{kg mol}}{\text{s}}. \tag{6.7}$$

In view of Eqs. (2.4) and (6.6) we obtain the mole flowrate of F_2 required to provide the full burnout of UO_2:

$$\text{Mo}_f(F_2) = 3\text{Mo}_f(UO_2) = 7.278 \times 10^{-4} \frac{\text{kg mol}}{\text{s}}. \tag{6.8}$$

The inlet mole fractions of F_2 and Ar are taken equal to 0.9 and 0.1 respectively. This means that the mass fractions of these gases at the inlet are equal to

$$M_F(F_2) = \frac{0.9M(F_2)}{0.9M(F_2) + 0.1M(Ar)} = 0.895, \tag{6.9}$$

$$M_F(Ar) = 0.105 \tag{6.10}$$

and are practically unaffected by the presence of particles.

Firstly we assumed that the gas temperature at the inlet is equal to the room temperature, i.e., 293 K. The results of our computations in this case turned out to be negative in the sense that the reaction could not properly develop. Non-reacting particles with temperatures under 350 K escaped through the outlet. The reaction might eventually have developed but only after executing many more iterations and particle tracking calculations. An alternative explanation is that local fluctuations of temperature were not accounted for in our computations. Such fluctuations may trigger the reaction.

Table 3
The piecewise linear fit for C_p of UO_2

Temperature (K)	Specific heat (J/mol K)	Specific heat (J/kg K)
300	65	240.7
400	70	259.3
600	78	288.9
700	82	303.7
1000	84	311.1
1400	85	314.8
1600	86	318.5
2000	100	370.4
2400	120	444.4
2670	167	618.5
3000	167	618.5

In order to illustrate the performance of our code we consider another extreme case when the gas enters the enclosure at a higher temperature equal to 800 K, so as to provide favourable conditions for triggering the reaction.

Assuming that the total gas pressure p_T is equal to 1 atmosphere and the gas temperature $T = 800$ K, we can obtain from Eqs. (6.7) and (6.8) the value of gas velocity necessary to provide the required mole flowrate of F_2:

$$v_0 = \frac{\mathrm{Mo_f}(F_2) N_A k_B T}{0.9 p_T S}, \tag{6.11}$$

where

$$p_T = 1.013 \times 10^5 \text{ N/m}^2, \quad k_B(\text{Boltzmann constant}) = 1.381 \times 10^{-23} \text{ J/K}, \quad T(\text{Initial particles temperature}) = 800 \text{ K},$$
$$N_A(\text{Avogadro number}) = 6.02 \times 10^{26} \text{ molecules/kg mol}, \quad S(\text{area of the inlet}) = 0.0324 \text{ m}^2. \tag{6.12}$$

Having substituted Eqs. (6.8) and (6.12) into Eq. (6.11) we obtain

$$v_0 = \frac{1.803 \times 10^3}{0.9117 \times 3.24 \times 10^3} = 1.638 \text{ m/s}. \tag{6.13}$$

We assume that the particles at the inlet have the same initial velocity.

The value of specific heat C_p has been approximated by a piecewise linear function based on results reported by Fink [12] and Gotta and Philipponneau [13]. The piecewise linear fit for C_p of UO_2 is presented in Table 3.

The value of the gas specific heat was considered to be composition dependent with $C_p(Ar) = 5$ cal/mol K = 523 J/kg K; $C_p(F_2) = 9$ cal/mol K = 991 J/kg K (see Kuo [5]). The value of C_p for fictitious gas UF_6O_2 was computed from the equation

$$C_p\left(\frac{\text{J}}{\text{kg K}}\right) = \frac{C_p(O_2)\ \text{J/kg mol K} + C_p(UF_6)\ \text{J/kg mol K}}{M(O_2)\ \text{kg/kg mol} + M(UF_6)\ \text{kg/kg mol}} = \frac{32000 + 150000}{32 + 352} = 474\ (\text{J/kg K}). \tag{6.14}$$

As mentioned in Section 2, there are no experimental data for the reaction rate at temperatures above 800 K. This leaves us some freedom in extrapolating the reaction rate in this temperature range. We assume that the reaction rate determined by Eq. (2.8) is valid in the temperature range up to T_{up} and remains constant at higher temperatures. In fact we can expect that at temperatures approaching 2000 K the reaction rate decreases due to dissociation of UF_6 molecules (see Tumanov and Tsirel'nikov [14])). We cannot, however, quantify either the rate of this decrease or the temperature when the reaction rate reaches its maximum at the moment.

6.2. Results of computations

Firstly we present the results of the computations for the case when the contribution of particles can be ignored (Section 6.2.1). Then we present the results of our self-consistent solution, assuming that the initial particle diameter D_{p0} is equal to 5×10^{-5} m (Section 6.2.2).

6.2.1. Contribution of particles is ignored

Since the contribution of particles was ignored, the problem reduces to a calculation involving only a mixture of Ar and F_2. From our computations follows the expected result that the mass fractions of these gases remain constant. In Fig. 4 we

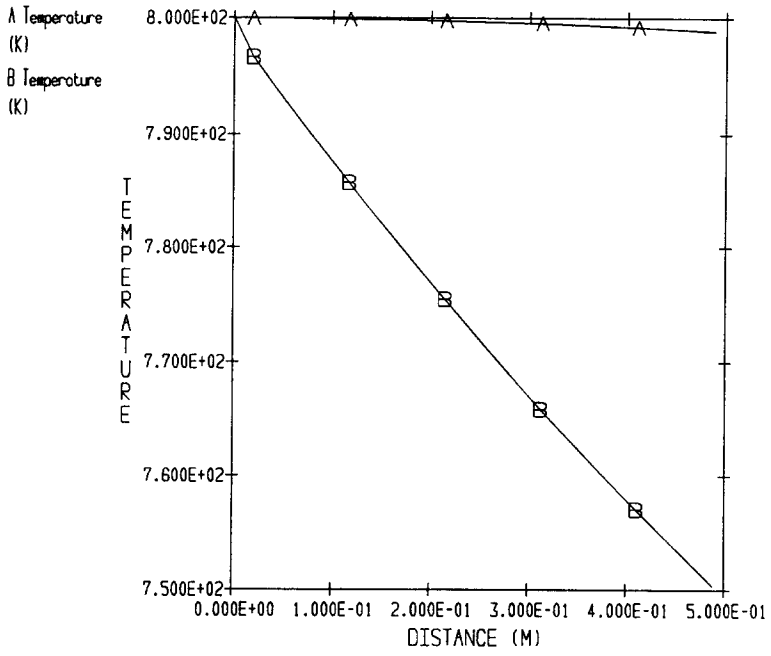

Fig. 4. Plots of temperature versus distance along the pipe on the assumption that the contribution of particles can be ignored. Plot A refers to the centre of the pipe while plot B refers the near wall area.

presented the plot of temperature versus distance near the centre line (curve A) and near the wall (curve B). As follows from this figure, the temperature drops more quickly near the walls than at the centre line. This result could be expected as heat is gradually removed through the walls of the enclosure. The same plots but for the parallel gas velocity show the slight increase of this velocity near the centre line follows from the conservation of mass flowrate and the reduction in parallel velocity near the wall.

6.2.2. Flow with particles

The plots of mass fractions for the four gases Ar, F_2, UF_6 and O_2 versus distance are shown in Fig. 5. As can be seen from this figure, the mass fraction of F_2 drops from 90% to almost zero at the distance near 1 m, which is consistent with the fact that all the uranium dioxide has fully reacted inside the enclosure. The mass fractions of UF_6 and O_2 (products of reaction) on the other hand increase from zero to just below 90% and 10% respectively. The mass fraction of Ar decreases from about 10% to less than 5% due to the increased contribution of UF_6 and O_2. As can be seen from this figure, the reaction takes place in a very localized part of the enclosure, rather than in the whole enclosure. This can be understood at a qualitative level: the reaction is accompanied by a considerable release of heat and this heat in its turn accelerates the reaction (see Eq. (2.7)).

This explanation is confirmed by the plots of gas temperature versus distance as shown in Fig. 6 for the region near the centre line and near the wall. As can be seen from this figure, at distances close to 1 m this temperature increases very quickly due to the heat released in the process of reaction. For larger distances this temperature drops gradually due to the removal of heat through the walls (cf. Fig. 4).

In Fig. 7 we present plots of the distance reached by the particle at a given time versus time. Most plots terminate at the distance near 1 m, where all the particles except those in the immediate vicinity of the walls have been converted to gaseous products. This distance corresponds to that where the concentration of UF_6 and O_2 (products of reaction) increases sharply as shown in Fig. 5.

In Fig. 8 we present plots of particle diameter versus time for five different injections. In all cases particle diameters decrease sharply over very short periods of time, which is consistent with the vigorous nature of the reaction as discussed earlier. In the case of particles in the immediate vicinity of the walls we observe a slow down of the reaction in spite of high temperatures. This is explained by the depletion of concentration of F_2 in this region. The turbulent diffusion of F_2 from other areas of the domain is reflected in the erratic behaviour of particles' diameter with time.

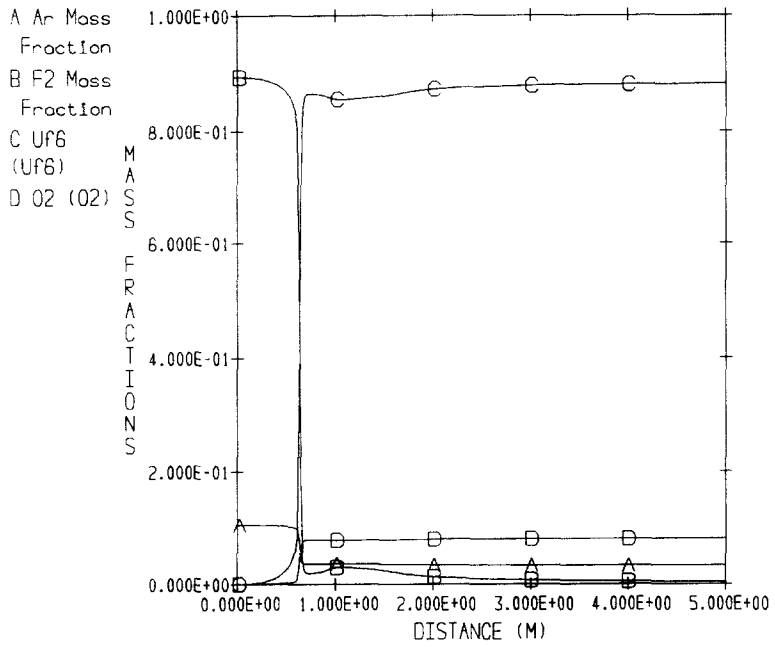

Fig. 5. Plots of mass fractions of Ar, F_2, UF_6 and O_2 versus distance along the pipe on the assumption that the initial particle diameter D_{p0} is equal to 5×10^{-5} m.

Note that the particle temperature is very close to the gas temperature as expected. The corresponding plots of temperature versus time have not been reproduced.

In the case when particles' diameter is reduced to $D_{p0} = 5 \times 10^{-6}$ m the reaction takes place at distances close to zero,

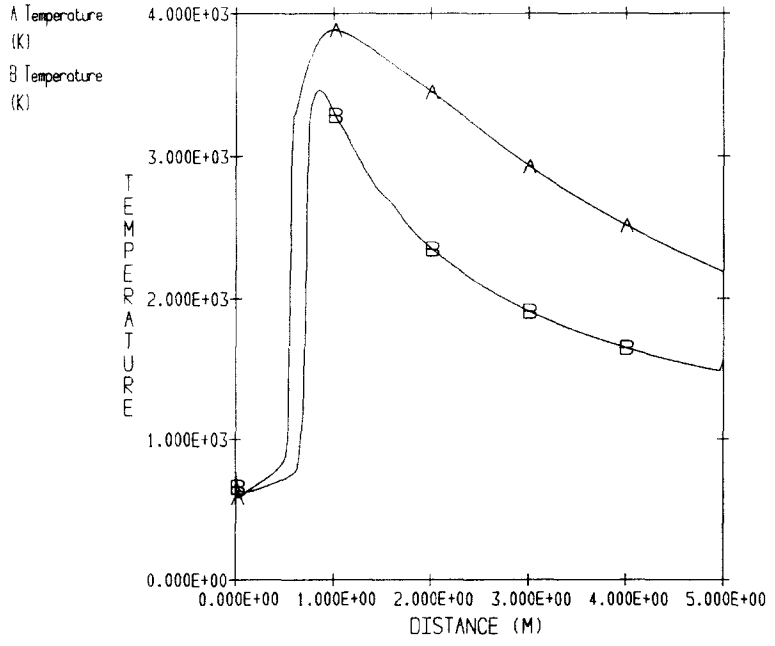

Fig. 6. Plots of gas temperature versus distance along the pipe near the axis (curve A) and near the wall (curve B) on the assumption that the initial particle diameter D_{p0} is equal to 5×10^{-5} m.

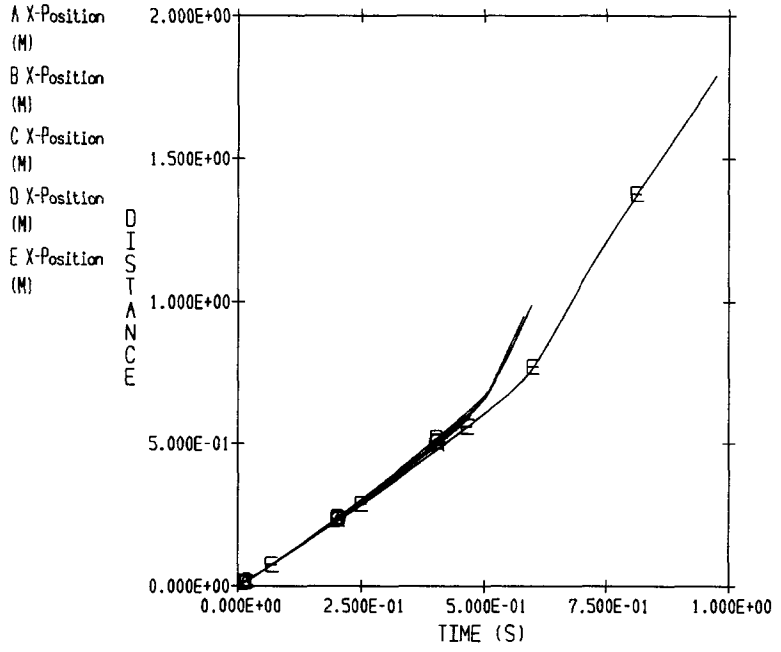

Fig. 7. The distance at which particles are located versus time for five injections on the assumption that the initial particle diameter D_{p0} is equal to 5×10^{-5} m.

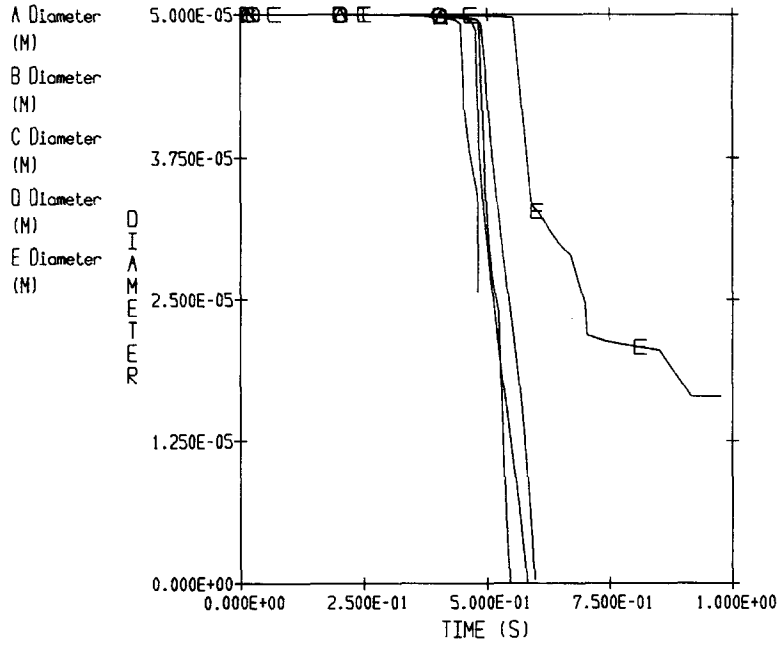

Fig. 8. Particle diameters versus time for five injections on the assumption that the initial particle diameter D_{0p} is equal to 5×10^{-5} m.

which is rather different from the case shown in Fig. 8. This reflects the fact that smaller particles have a larger surface area per unit volume, which creates better conditions for a rapid surface reaction.

7. Conclusions

A detailed analytical study of the equations describing the fluorination of UO_2 particles is presented for some limiting cases. The analytical solutions obtained can be used for approximate estimates of the effect of fluorination on particle

diameter and temperature provided that the mass flowrate of these particles is so small that they do not affect the state of the gas. Their major application, however, is probably in the verification of self-consistent numerical solutions.

It has been shown that in the limiting cases for which analytical solutions have been derived, the coincidence between numerical and analytical results is almost exact. This can be considered as a verification test for both these solutions.

Computational results are presented and discussed for a self-consistent problem in which both the effects of gas on particles and particles on gas are accounted for.

Acknowledgements

Authors are grateful to BNFL for financial support. Special thanks are to E.M. Sazhina and O. Faltsi-Saravelou for their help with the coding work and useful advices.

References

[1] T. Yahata, M. Iwasaki, J. Inorg. Nucl. Chem. 26 (1964) 1863.
[2] M. Iwasaki, J. Nucl. Mater. 25 (1968) 216.
[3] T. Sakurai, J. Phys. Chem. 78 (1974) 1140.
[4] T. Sakurai, Japan Atomic Energy Research Institute Report No. 1243, 1976.
[5] K.K. Kuo, Principles of Combustion (Wiley, New York, 1986).
[6] G.C. Pomraning, G.M. Foglesong, J. Comput. Phys. 32 (1979) 420.
[7] R.B. Bird, W.E. Stewart, E.N. Lightfoot, Transport Phenomena (Wiley, New York, 1960).
[8] L.D. Landau, E.M. Lifshitz, Fluid Mechanics (Pergamon, Oxford, 1987).
[9] R. Siegel, J.R. Howell, Thermal Radiation Heat Transfer (Hemisphere Publishing Corporation, Washington, 1992).
[10] S.S. Sazhin, E.M. Sazhina, O. Faltsi-Saravelou, P. Wild, Fuel 75 (1996) 289.
[11] I.S. Gradstein, I.M. Ryzhik, Tables of Integrals (Fizmatgiz, Moscow, 1962) (in Russian; English translation is available).
[12] J.K. Fink, Int. J. Thermophys. 3 (1982) 165.
[13] M.J. Gotta, Y. Philipponneaux, Trans. Am. Nucl. Soc. 66 (1992) 179.
[14] Yu.N. Tumanov, K.V. Tsirel'nikov, Phys. Chem. Mater. Treat. 26 (1992) 541.